energies

MDPI

Review

Metamaterial-Based Radiative Cooling: Towards Energy-Free All-Day Cooling

Byoungsu Ko [1,2], Dasol Lee [2], Trevon Badloe [2] and Junsuk Rho [2,3,*]

1 Department of Mechanical Engineering, Myongji University, Yongin 17058, Korea; 60152260@mju.ac.kr
2 Department of Mechanical Engineering, Pohang University of Science and Technology (POSTECH), Pohang 37673, Korea; dasol2@postech.ac.kr (D.L.); trevon@postech.ac.kr (T.B.)
3 Department of Chemical Engineering, Pohang University of Science and Technology (POSTECH), Pohang 37673, Korea
* Correspondence: jsrho@postech.ac.kr; Tel.: +82-54-279-2187

Received: 12 November 2018; Accepted: 15 December 2018; Published: 28 December 2018

Abstract: In the light of the ever increasing dangers of global warming, the efforts to reduce energy consumption by radiative cooling techniques have been designed, but are inefficient under strong sunlight during the daytime. With the advent of metamaterials and their selective control over optical properties, radiative cooling under direct sunlight is now possible. The key principles of metamaterial-based radiative cooling are: almost perfect reflection in the visible and near-infrared spectrum (0.3–3 μm) and high thermal emission in the infrared atmospheric window region (8–13 μm). Based on these two basic principles, studies have been conducted using various materials and structures to find the most efficient radiative cooling system. In this review, we analyze the materials and structures being used for radiative cooling, and suggest the future perspectives as a substitute in the current cooling industry.

Keywords: metamaterial; daytime radiative cooling; infrared atmospheric window; selective reflection; selective emission

1. Introduction

As the awareness of the dangers of global warming grows, many novel ideas are being put forward to prevent the problem from developing further. Lots of research has been performed to find the method of cooling that minimizes the amount of air pollution and energy consumption in buildings, vehicles, and clothing [1–3]. Recently developed approaches are focused on radiative cooling, a technique requiring no energy to lower the ambient temperature, thus considered as a key to help to slow down the disastrous effects of global warming. Radiative cooling is a way of radiating heat into the universe using the transparency window of the Earth's atmosphere (8–13 μm).

Various nighttime radiative cooling research has been reported by constructing selective emitters in the atmospheric transparency window [4–6] but the same techniques are inefficient during the daytime under strong sunlight. Daytime radiative cooling requires the additional condition of reflecting the entire solar spectrum (0.3–3 μm), while maintaining enough thermal radiation in the atmospheric window (Figure 1a) [7–9]. The biggest hurdle is that the absorption of solar energy usually far exceeds the possible thermal radiative power [9–17]. Metamaterial-based radiative cooling achieves sufficient daytime cooling by being designed to satisfy those exact conditions. Metamaterials are artificial structures which can realize various optical properties that do not exist in nature and have been developed with the advancement of high-level nanofabrication methods to create perfect absorbers, reflectors and spectral filters [18–23]. Metamaterial-based radiative cooling entered a new phase after influential research by Raman et al. [14,24,25] optimized the structure design to have optical

properties that reflect the solar spectrum and emit thermal energy in the infrared (IR) atmospheric window [26,27]. Daytime radiative cooling was demonstrated with a decrease of 4.9 °C below the ambient temperature (cooling power: 40.1 W/m^2) [28]. Follow-up studies have begun to research various shapes and structures of metamaterial-based radiative cooling methods [28–30], including biomimetics and the painting of metamaterials directly onto a surface [31,32]. Radiative cooling using phase change materials has also shown the additional function of temperature-dependent smart switching [33].

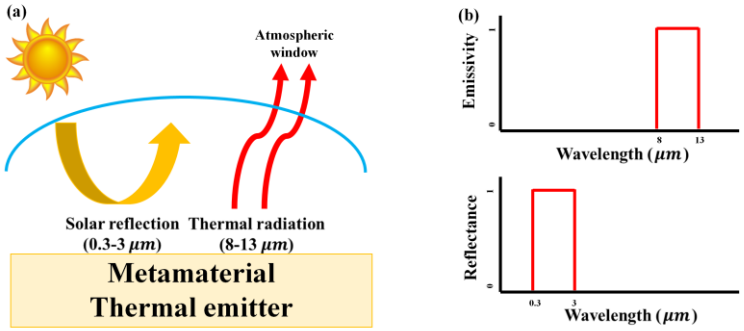

Figure 1. Schematic of the main concepts of metamaterial-based radiative cooling. (**a**) Schematic of the basic principles of radiative cooling. (**b**) Ideal reflection and emission properties for radiative cooling.

In this review, we discuss recent theoretical and experimental developments of radiative cooling techniques as an arising tool for energy-free all-day cooling, focusing on the structures and materials. We briefly describe the basic concepts and mechanisms needed to realize radiative cooling. Then we provide details of various investigations based on their experimental results from each structure and material. Finally, we provide the future perspectives and a discussion of radiative cooling. We expect this review to deliver insight into the concepts of radiative cooling and explore the advanced functionalities and applications which are useful for the cooling industry, such as in buildings, vehicles, and the functional clothing industry.

2. Principles of Radiative Cooling

2.1. Basic Theory

To realize radiative cooling, two main concepts should be understood. First, from thermodynamics, it is known that heat will spontaneously flow from a hot to a cold body. Therefore, heat from high-temperature terrestrial bodies (~300 K) can always flow towards a low-temperature sink, the biggest and lowest of all being outer space (3 K) [29]. Second, there is a transparent window in the atmosphere (8–13 μm) that can be used to exchange heat between the Earth and outer space in the form of infrared radiation. Radiative cooling exploits these concepts to achieve energy-free cooling. An ideal radiative cooling system would have 100% reflectance over the whole solar spectrum while simultaneously having 100% thermal emission in atmospheric window (Figure 1b). By optimizing a metamaterials design these two conditions can be satisfied, so passive, energy-free cooling can be achieved.

2.2. Appropriate Conditions and Related Formula

The important parameters for radiative cooling power are: the radiating materials area A, temperature T, spectral and angular emissivity $e(\lambda, \theta)$, and the ambient temperature T_{amb}. The net radiative cooling power, $P_{n \cdot r \cdot c}$ Pcoolcan be expressed as:

$$P_{n \cdot r \cdot c}(T) = P_{rad}(T) - P_{atm}(T_{amb}) - P_{sun} - P_{c \cdot d + c \cdot v} \quad (1)$$

The radiated power from thermal emission in the atmospheric window, $P_{rad}(T)$, can be expressed as:

$$P_{rad}(T) = A \int d\Omega \cdot \cos\theta \int_0^\infty d\lambda \cdot I_{B \cdot B}(T, \lambda) \cdot e(\lambda, \theta) \quad (2)$$

where $\int d\Omega = 2\pi \int_0^{\pi/2} d\theta \sin\theta$ is the angular integral over a hemisphere, $I_{B \cdot B}(T, \lambda) = (2hc^2/\lambda^5) \cdot \left[e^{hc/\lambda k_B T} - 1\right]^{-1}$ is the spectral radiance of a blackbody at temperature T, h is Planck's constant, k_B is the Boltzmann constant, c is the speed of light in vacuum, and λ is the wavelength.

The absorbed power from the opaque atmospheric thermal radiation, $P_{atm}(T_{amb})$, can expressed as:

$$P_{atm}(T_{amb}) = A \int d\Omega \cdot \cos\theta \int_0^\infty d\lambda \cdot I_{BB}(T_{amb}, \lambda) \cdot e_{atm}(\lambda, \theta) \quad (3)$$

While the solar power absorbed by the device, P_{sun}, can be expressed as:

$$P_{sun} = A \int_0^\infty d\lambda \cdot e(\lambda, \theta_{sun}) \cdot I_{AM1.5}(\lambda) \quad (4)$$

where $I_{AM1.5}(\lambda)$ is the solar illumination intensity. Using Equations (3) and (4) and applying Kirchhoff's law of thermal radiation, i.e., substituting absorptivity with emissivity, the angle dependent atmosphere emissivity $e(\lambda, \theta)$ can be expressed as:

$$e_{atm}(\lambda, \theta) = 1 - t(\lambda)^{1/\cos\theta} \quad (5)$$

where $t(\lambda)$ is the atmospheric transmissivity in the zenith direction. The power loss caused by heat transfer through conduction and convection can expressed as:

$$P_{c \cdot d + c \cdot v}(T, T_{amb}) = A h_{tot}(T_{amb} - T) \quad (6)$$

where h_{tot} is the combination of the non-radiative heat coefficients, $h_{c \cdot d}$ (conduction) and $h_{c \cdot v}$ (convection), which occur from the contact between the radiative cooling material and the external surface.

$P_{n \cdot r \cdot c}(T)$ is the total net radiative cooling power calculated by subtracting the power that flows into the cooler from the power that is radiated out. Energy-free daytime radiative cooling is achieved when the heat radiated out to space is larger than the heat absorbed from the sunlight, atmospheric radiation, and other non-radiative mechanisms. In order to optimize the radiative cooling power, it is necessary to minimize P_{sun}, P_{atm}, and $P_{c \cdot d + c \cdot v}$, while selectively emitting thermal radiation in the transparent atmospheric window to maximize P_{rad}.

3. Photonic Metamaterials for Real-Life Applications

3.1. Metamaterial-Based Radiative Cooling Using a Film Structure

Raman et al. [28] used a one-dimensional photonic film consisting of seven alternating layers of hafnium dioxide (HfO_2) and silicon dioxide (SiO_2) of varying thicknesses on top of a 200 nm silver (Ag) substrate (Figure 2a). This radiative cooling film, consisting of one reflective layer and one emissive layer, was able to achieve cooling to 4.5 °C below the ambient temperature, proving the feasibility of daytime radiative cooling. Film-format radiative cooling has been an active research topic since 2014, with many advances shown in Reference [34]. Subsequent studies selected other materials to find the optimum elements for radiative cooling. Chen et al. [29] utilized layers of silicon nitride (Si_3N_4), silicon (Si), and aluminum (Al) components (Figure 2b) to achieve an ideal selective thermal emitter in the atmospheric window. Importantly, by placing their device in a vacuum chamber that was shielded from direct sunlight, all parasitic losses from conduction and convection from the air, and radiation and conduction from the back of the device itself were minimized to almost zero. On average, a 37 °C

temperature reduction below ambient was achieved. The final film-type structure [35] was constructed with layers using all the key elements from previous research [36]. This film was made up of multiple layers of SiO_2 and titanium dioxide (TiO_2) on an Al or Ag layer (Figure 2c), thereby consisting of low- and high-index materials to utilize their emission spectra and high absorption caused by the phonon-polariton resonance. Using this simple, easy-to-manufacture layered film design, the ability to lower the temperature to 5 °C below ambient with a radiative cooling power of 100 W/m^2 was demonstrated. These studies showed that the thickness of the emissive layer is important, and the surrounding environment plays a key role in cooling power.

The next generation of research was carried out in a new paradigm, with the concept of introducing a dielectric spacer. By having a lossless dielectric spacer, the photonic bandgap can be regulated to perform wavelength-selective, temperature-modulated emission. The earliest research consisted of thermally switchable vanadium oxide (VO_2) and Al on either side of a dielectric spacer [37] (Figure 2d). When the temperature of the VO_2 is below 67.85 °C, the structure is highly reflective, thereby minimizing solar absorption. On the other hand, above 71.85 °C the VO_2 acts as a metal and forms a Fabry–Perot cavity with a high, broadband emissivity around the atmospheric window region, providing a radiative cooling effect due to the enhanced thermal emission. The radiative power increases from 38 W/m^2 to 242 W/m^2 after the VO_2 phase transition. Both wavelength-selective and temperature-modulated emittance were shown.

The subsequent research focused on daytime radiative cooling using polymers. The first experimental demonstration of radiative cooling using polymers [38] consisted of a 4 inch, 500 μm thick SiO_2 wafer with a 100 μm thick polydimethylsiloxane (PDMS) film as a top layer and a 120 nm thick Au film as a back reflector (Figure 2e). The PDMS layer is transparent to the wavelengths needed to be reflected and emits over a range larger than the atmospheric window. Although it absorbs extra atmospheric radiation, it was shown that at lower temperatures, cooling resulting in a drop of 8.2 °C below ambient temperature under direct sunlight can be achieved. The following studies by Yang et al. [39] demonstrated radiative cooling consisting of a polytetrafluoroethylene (PTFE) and Ag film on Si (Figure 2f). Through the high reflectance of PTFE, from ultraviolet to near-IR wavelengths (0.2–2.5 μm), in combination with the reflecting metal and the emitting Si, radiative cooling to 11 °C below the ambient temperature was achieved. High humidity limits the emission power as it closes the atmospheric window. To investigate the effects of humidity, Suichi et al. [40] used a film consisting of four layers (Figure 2g), an Al layer that acts as a mirror and the remaining layers selected based on phonon resonances. SiO_2 serves to selectively emit thermal radiation in the atmospheric window, while the top SiO_2 and polymethyl methacrylate (PMMA) layers are designed to optimize the multiple interference effects for enhanced thermal radiation. Although this research could not overcome the problems that warm and humid conditions cause for daytime radiative cooling, their research offered a perspective solution for practical applications in warm and humid areas. Namely, by only maximizing thermal radiation in the first atmospheric window and by minimizing radiation everywhere else, including the second atmospheric window (at 16–25 μm) as high humidity acts to close this window completely. In using polymers for radiative cooling, the polymer layer plays an important role in assisting the conventional reflection and emission layers.

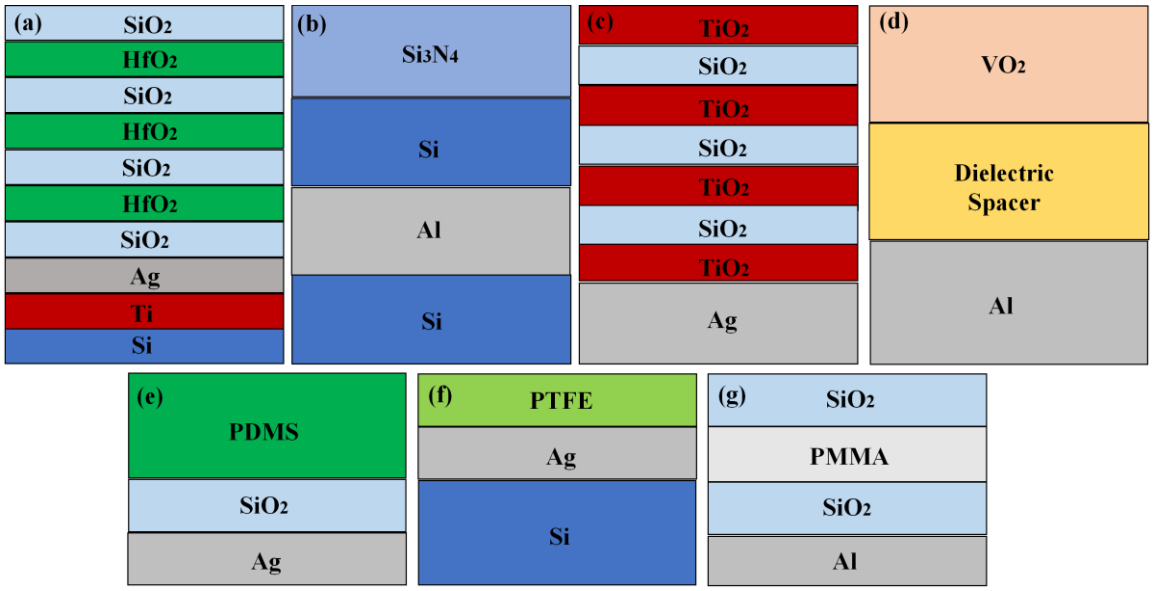

Figure 2. Schematics of various metamaterial film structures used for radiative cooling. Each design has a different layered structure: (**a**) HfO_2/SiO_2 multi-layer on Ti [28], (**b**) $Si_3N_4/Si/Al$ on Si [29], (**c**) SiO_2/TiO_2 multi-layer on a metallic Al/Ag reflector [35], (**d**) VO_2 with a dielectric spacer on Al [37], (**e**) PDMS/SiO_2 on Ag [38], (**f**) PTFE/Ag on Si [39], and (**g**) SiO_2/PMMA/SiO_2 on Al [40] have been reported.

3.2. Metamaterial-Based Radiative Cooling Using Nanostructures

Nanophotonic structures can be designed to prevent sunlight absorption by increasing the reflectance in the sunlight-concentrated spectrum (0.3–3 μm) and can be simultaneously designed for maximum emissivity in the atmospheric window (8–13 μm). Raphaeli et al. [41] suggested the possibility of daytime radiative cooling with a nanophotonic structure. The design was comprised of two thermally emitting photonic crystal layers of silicon carbide (SiC) and quartz on top of a broadband solar reflector consisting of bilayers of magnesium fluoride (MgF_2) and TiO_2 with varying periods, on an Ag substrate (Figure 3a). The dielectric layer acts as a reflector which minimizes solar absorption while the 2D photonic crystal structure acts as a selective thermal emitter. This design showed a decrease of almost 5 °C below the ambient air temperature. Zhu et al. [42] used an SiO_2 photonic crystal absorber for radiative cooling (Figure 3b). Silicon oxide was chosen because it exhibits a strong phonon-polariton resonance in the atmospheric window region. The absorber was a square-lattice photonic crystal with a periodicity of 6 μm, made by etching 10 μm-deep air holes into a double-sided 500 μm polished fused silica wafer. When placed under direct sunlight, this device managed to reduce the temperature by 13 °C from ambient.

The first research on antenna type structures was carried out by Hossain et al. [43], where a conical-shaped, anisotropic, multilayer metal dielectric metamaterial (CMM) was used (Figure 3c). The CMM pillars consisted of alternating layers of germanium (Ge) and Al on an Si substrate. By selecting Ge and Al, the CMM pillars have dispersive properties and anisotropic, ultra-broadband, spectrally selective, near unity absorption of unpolarized light [32,44–47]. As a result, a reduction of 12.2 °C below the ambient temperature under direct sunlight was achieved. Wu et al. [48] followed up this research by designing two-dimensional antenna composed of a low-loss alternating aluminum oxide (Al_2O_3) and SiO_2 multi-layer structure (Figure 3d). This exhibits near ideal unity IR emissivity and solar reflection. This design can theoretically obtain a tremendous radiative cooling effect of 47 °C below the ambient temperature but is complicated to fabricate. The most recent research using antenna structures by Cho et al. [30] demonstrated thermal radiation using different materials. Tungsten (W) thermal emitters have a high emissivity over a broad range of wavelengths and angles, and maintain this property at temperatures up to 1300 K (Figure 3e). They found that as the aspect ratio of the cone

increases, the emission improves. Radiative cooling using W on the Earth is possible, but it is likely to be more useful for applications where extreme heat-resistance is needed, such as space travel. However, the most important aspect of this research was the novel use of laser interference lithography (LIL) for fabrication. Laser interference lithography has advantages such as high throughput, large-scale manufacturing possibilities, cost-effectiveness, and cleanliness [49–51], all of which have a considerable influence on the possible commercialization of radiative cooling applications.

A simple structure is important for the commercialization of radiative cooling [52,53]. Zou et al. [54] demonstrated the simplest radiative cooling structure which consists of a two layered metasurface (Figure 3f). A phosphorus-doped n-type silicon substrate was used for the required emissivity at IR frequencies. To enhance the emissivity and reflect the unwanted solar radiation, the Ag layer and doped silicon formed a dielectric resonator (DR) metasurface. Powerful cooling was realized by using the magnetic dipole resonance of the DR to achieve wide-angle broadband emission in the atmospheric window. This design showed a temperature decrease of 10.29 °C and 7.36 °C for night and daytime radiative cooling, respectively. Qu et al. [55] demonstrated a tunable nanodisk double-band thermal emitter made from the phase change material $Ge_2Sb_2Te_5$ (GST) (Figure 3g). They showed that as the GST is tuned from its amorphous to crystalline phase, two thermal emission peaks can be tuned, one at 5.4–7.36 μm and one at 7.56–10.01 μm. The advantage of using phase change properties is that the same structure can be used for radiative cooling in two different atmospheric window regions (3–5 μm and 8–13 μm). Follow-up research by Sun et al. [56] used aluminum-doped zinc dioxide (AZO), SiO_2, Al, and Si. Aluminum-doped zinc dioxide was selected for its properties as a transparent conducting oxide that can achieve a plasmonic response in the IR region (Figure 3h). More recently, Hervé et al. [57] and Liu et al. [58] created designs to control the thermal emission spectrally and directionally using gratings that can regulate the surface phonon-polariton resonance. The focus was on the thermal control of gratings on multi-layer structures that consist of boron nitride (BN), SiC, and SiO_2 [57] (Figure 3i). This structure has an emissivity peak in the atmospheric window and near perfect reflectivity over the solar spectrum. Using a 2D grating with emission peaks of around 100% for unpolarized light and emission at all angles, a decrease to 5 °C below the ambient temperature was achieved. Wu et al. [59] used a VO_2 and SiO_2 grating to create a thermally switchable Fabry–Perot-like cavity (Figure 3j). By optimizing the geometric parameters of the metamaterial and controlling the temperature of the phase change material, the emission peak can be tuned to the atmospheric window. The radiative cooling power can be thermally controlled to produce a four-fold increase when the device temperature is above the phase change temperature of VO_2. Using this property, VO_2 has shown the ability of passive smart switching, i.e., increasing the cooling power at higher temperatures.

Jia et al. [60] demonstrated radiative cooling using nanospheres. A polarization-independent double-layer nanoparticle crystal with emission in the near-IR region was designed (Figure 3k). If the metallic nanoparticle crystal can be properly oxidized, a natural dielectric layer can be formed which results in an enhancement of the selective emission in the atmospheric window.

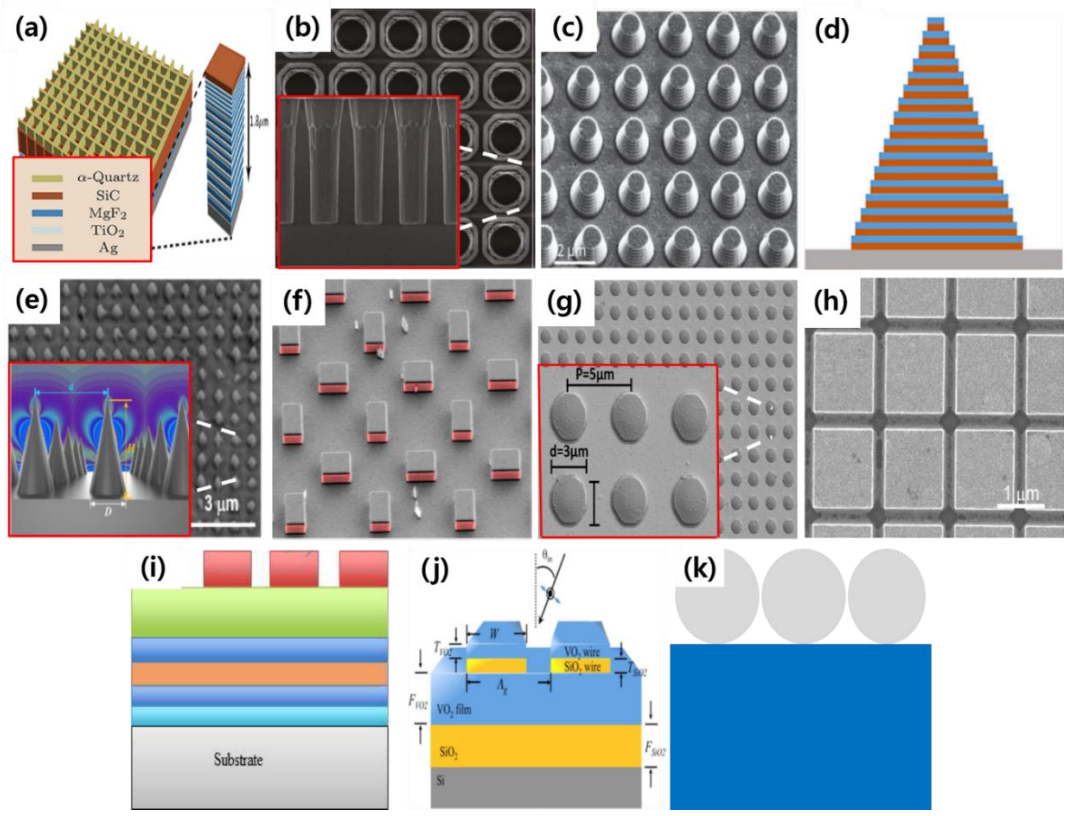

Figure 3. Various metamaterial-based radiative cooler structures: (**a**) metal-dielectric lattice structure [41], (**b**) photonic crystal structure [42], (**c**) conical shape array [43], (**d**,**e**) antenna structures [30,48], (**f**–**h**) metasurfaces [54–56], (**i**,**j**) gratings [57,59], and (**k**) sphere arrays [60] have been reported.

3.3. Metamaterial-Based Radiative Cooling Using Random Particles

Most of the previous studies have focused on proving the concept of and improving the efficiency of radiative cooling. However, after the feasibility of efficient daytime radiative cooling had been proven, methods of using random particles to increase the manufacturing speed and cost efficiency in the light of commercialization have been proposed [61,62]. The concept of random particles for radiative cooling uses the nanosphere design introduced in the previous section; however, by arranging the nanospheres randomly, the need for complicated structures and precise fabrication disappears. Gentle et al. [63] conducted research consisting of a top layer of a mixture of SiC and SiO_2, selected for their emissivity in the atmospheric window and a bottom layer made up of an Al plate to reflect solar radiation (Figure 4a). Bao et al. [7] showed that by using densely packed TiO_2 particles on top of densely packed SiC or SiO_2 particles, all on an Al substrate can be used for radiative cooling purposes (Figure 4b). This design was able to produce an 8 °C reduction below the ambient temperature in a region with high humidity. The subsequent experiments were conducted with coatings that added extra elements to existing emitters to achieve better selective emissivity. Hueng et al. [64] used a simple double-layer design consisting of an acrylic resin embedded with TiO_2 and black carbon particles (Figure 4c). The emissivity of single nanospheres was calculated and TiO_2 particles with radii of 0.2 μm were found to be the optimum size, with important properties of 90% reflectance and around 90% emissivity. Using this design, the emissivity of a surface can be greatly improved by applying the coating. This random-particle embedded coating can theoretically decrease the temperature from ambient to 22 °C and 45 °C, at daytime and nighttime respectively.

Lu et al. [65] applied a unique fabrication method of modified silica sol-gel imprinting, which makes it possible to increase the durability of the device for real-life applications (Figure 4d) with an

average emissivity measured to be greater than 96% in the atmospheric window region. This method could be utilized in radiative cooling applications such as textiles [66–68]. Fu et al. [69] complemented the previous research by utilizing a manufacturing method that is suitable for mass production. A porous anodic aluminum oxide membrane made using fast and scalable chemical methods was proposed (Figure 4e). This membrane has high emissivity in the atmospheric window with almost 0% absorption over the solar spectrum. Aluminum was chosen for the porous random structure due to having a highly acoustic resonance in the atmospheric window. Air holes made in the chemical reaction can also help to decrease the dielectric constant of the material, therefore improving the impedance matching with the surrounding air [70]. This design was used to produce a modest 2.6 °C reduction of the temperature below ambient. Using this manufacturing method, inexpensive, and large-scale radiative cooling can be achieved.

Zhai et al. [71] and Zhang et al. [72] demonstrated efficient day and nighttime radiative cooling using a randomized, glass-polymer hybrid metamaterial consisting of SiO_2 microspheres randomly distributed in the matrix material of polymethylpentene (PMP) (Figure 4f). This kind of metamaterial, made by polymeric photonics is significantly growing in the field due to the attractiveness of its cost and large-scale manufacturing possibilities [10,15,24,46]. This polymer matrix metamaterial with encapsulated SiO_2 microspheres of ~4 μm has almost 0% loss in the solar spectrum. These experiments utilized a second atmospheric window (at 16–25 μm) for additional atmospheric radiation. The microspheres emit thermal energy through the atmospheric window due to strong Fröhlich phonon resonances. A 50 μm thick film containing a 6% volume of SiO_2 microspheres was fabricated. Backed with a 200 nm thick Ag coating, the film showed an average IR emissivity of over 93% and reflection of the solar irradiance of almost 96%. An average radiative cooling power of over 110 W/m^2 over the continuous 72 h experiment periods were recorded. With this average radiative cooling power, the device can cool to more than 10 °C below the ambient temperature, which is sufficient for commercialization. This design has several other advantages. It is possible to use roll-to-roll manufacturing to fabricate 300 mm wide sheets at a rate of 5 m/min, allowing for the application to large-scale surfaces such as cars and buildings. The polymer metamaterial is lightweight and easy to laminate on curved or geometrically complicated surfaces. Polymethylpentene also has excellent mechanical and chemical resistance, therefore suitable for outdoor use. Finally, the strongly scattering and non-specular optical response of this metamaterial will prevent back reflected glare, which can have fatal visual effects for people and interfere with airplanes.

At this point, most advanced radiative cooling methods are similar to the previous study in that they use PMP but are more suitable for real-life applications by being combined with paint. This is generally done by modifying the pigment components in commercial white solar reflective paint [14] to include 200–250 nm TiO_2 particles or hollow spheres of relatively low refractive index, with sizes ranging from 50 to 150 μm. However, these materials both have their inherent drawbacks for radiative cooling purposes; TiO_2 particles show high mid-IR emissivity but also high absorption of ultraviolet (UV) wavelengths which accounts for 5% of the total solar intensity, while the hollow spheres are not as good at scattering sunlight as TiO_2. Atiganyanun et al. [73] demonstrated that using low-index SiO_2 microspheres (Figure 4g) significantly outperformed commercial solar reflective white paint for daytime cooling. The low index particles maximize the optical scattering in the solar spectrum and enhance thermal emission in the atmospheric window; the solar radiation is dispersed in the microsphere coating, and heat is emitted from the surface through mid-IR emission. This microsphere-based coating on a black substrate can lower the temperature below ambient by about 12 °C in the daytime, without the need for expensive silver coatings. At peak performance, the SiO_2 microsphere coating achieves a substrate temperature that is 7 °C lower than commercial paint. The average temperature of the coated substrate is 4.7 °C lower than the average temperature of the substrate coated with commercial paints during intense solar radiation (11:00–16:00). At night (21:00–07:00) both the microsphere coating and the commercial paint keep the substrate temperatures about 4 °C below the ambient temperature. This result shows that the

two films have similar radiation properties at mid-IR, but the microsphere coating has excellent scattering properties in the solar spectrum compared to commercial paints. The most recently reported random particle-based radiative cooling technique by Mandal et al. [74] uses porous poly(vinylidene fluoride-co-hexafluoropropene) ($P(VdF\text{-}HFP)_{HP}$) (Figure 4h). In this research, by using a scalable phase inversion-based method, a simple to manufacture, inexpensive porous polymer-based radiative cooler was fabricated. The radiative cooling power of $P(VdF\text{-}HFP)_{HP}$ can lower the temperature to 6 °C below the ambient temperature and can be coated directly onto any existing material. The reported results are from microscale-sized spheres and fill fraction coatings, which are not yet fully optimized. After the particle size is optimized for sunlight scattering, even greater radiative cooling power under direct sunlight will be possible. In contrast to the previously discussed studies, the random particle-based techniques do not require expensive processing steps or materials and can be applied to almost any surface in a paint format. Therefore, this easy and scalable process, utilizing random particles, is a possibility for low-cost, easy-to-apply coatings that can be used for radiative cooling.

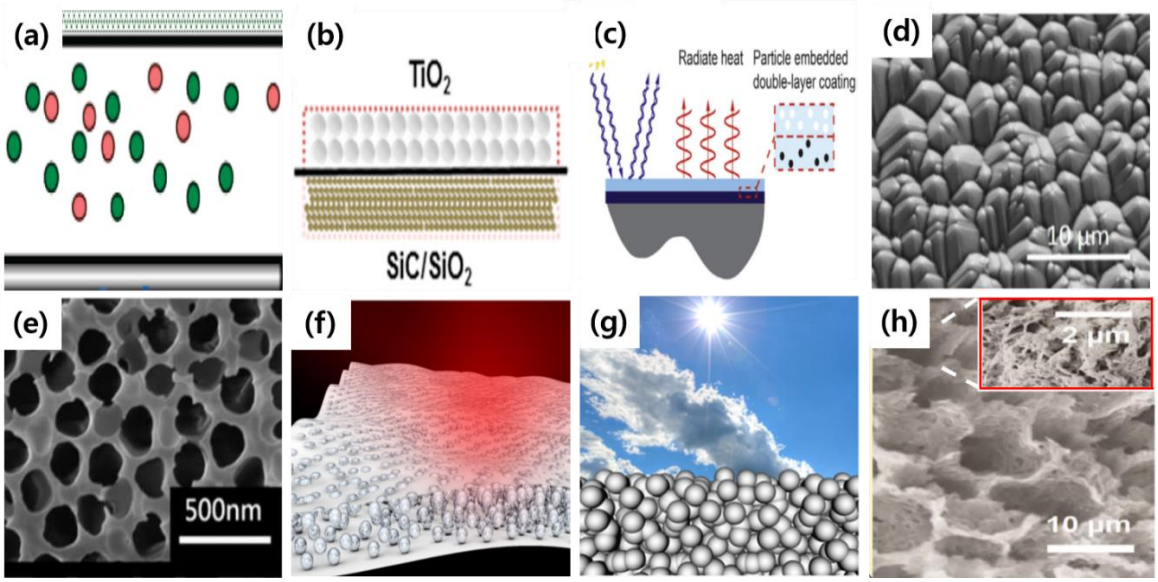

Figure 4. Various random particle-based designs for radiative cooling: (**a**,**b**) SiC/SiO_2 mixture [7,63], (**c**) acrylic resin in TiO_2 [64], (**d**) SiO_2 random antenna-shaped particles [65], (**e**) random porous structure [69], (**f**,**g**) SiO_2 microparticles [71,73], and (**h**) porous polymer [74] were reported.

4. Discussion and Perspective

Early research showed that photonic structures can be used for radiative cooling by optimizing their properties to achieve good selective spectral emissivity while using a metallic back reflector to reflect the solar irradiance. Simple layers of micro and nanoscale films were fabricated and tested to prove the concept of all-day radiative cooling. Cooling of around 5–10 °C was achieved by most of these simple designs. As an added degree of freedom, phase change materials were exploited for radiative cooling purposes. The GST can be used to selectively tune the emission into one of the two transparent atmospheric windows as the material changes from its crystalline to amorphous phase, allowing thermal control of the cooling power. The phase change between metal and insulator of VO_2 was used with a dielectric spacer layer to create either a broadband reflecting material or a Fabry–Perot cavity between the back reflector and the metallic VO_2, where the emission wavelength can be controlled by simply varying the thickness of the dielectric spacer. This allows the control of radiative cooling to be switched on or off at a specific temperature and could be an extremely useful technique to exploit in real-life situations.

By structuring the surface of nanophotonic materials, enhancements in the reflection and emission responses can be tailored for radiative cooling. A large variety of shapes and designs have been probed

to find the most effective solution. Nanorods, cones, disks, and gratings have all been utilized to prove the usefulness of nanophotonic designs for radiative cooling, demonstrating similar cooling powers as simple film-type structures, but with the added complexity comes an increase in the selectivity in the emission and reflection spectra, which can prove useful for areas with high humidity and adverse weather conditions. As a proof of concept, using a vacuum chamber to eradicate parasitic heat gains from the surrounding area and surfaces, all-day sub-zero cooling with an average temperature 37 °C below ambient have been shown. Photonic structures have been proved as a possible way to create all-day radiative cooling devices, they are inherently difficult to be applied to real-life situations due to the cost, lack of scalability, and difficulty of the fabrication techniques needed to produce them. At the moment, nanophotonic structures would need to be fabricated in labs using expensive, time-consuming, and difficult methods such as nanolithography, electron-beam lithography, and electron beam evaporation. This makes it almost impossible to simply add the desired radiative cooling properties to already existing, imperfect structures and materials as the substrates for the required fabrication methods should be flat. In addition, complex three-dimensional structure fabrication techniques are still lacking, which limits the complexity of the producible nanostructures. These boundaries on the production of nanophotonic-structure-based all-day radiative cooling are the key hurdles that must be overcome to allow the commercialization of this technology to consumers.

In just a few short years, new state-of-the-art radiative cooling technology has overcome these barriers by introducing random-particle-based methods that are easy to fabricate and apply to any surface. By introducing nanospheres into already existing solar radiation reflective paint, the emissive properties of the chosen material can be used to improve the cooling properties. As the addition of the nanospheres and the application of the paint to a surface basically create a random arrangement of the material, the size, material, and filling factor of the nanospheres should be optimized to improve the efficiency of this technique. Early studies have shown radiative cooling to around 10 °C lower than the ambient temperature, proving their worth as a radiative cooling method.

5. Conclusions

Energy-free all-day radiative cooling has been proven by using metamaterials as the base for the necessary selective emission and reflection spectra needed. Metamaterial-based radiative cooling in a variety of formats has been proven, from simple multilayer films and complicated nanostructured surfaces to randomly arranged nanospheres. Of all the methods reviewed here, the nanosphere design is the one of choice for future commercialization due to its large-scale production capabilities, and ease of fabrication and possibility of application to any existing surface. The choice of material and optimization of the nanosphere size and filling fractions need to be investigated more to produce the most efficient radiative cooling device possible. By using a paint-based format for the application of the nanospheres, large areas of uneven, rough, and even curved surfaces could be easily covered, so cars, buildings, and other large structures could benefit from the energy-free radiative cooling effect. More research into producing colorful paints would need to be done, which would inherently cause a loss of efficiency as the need for reflecting all solar irradiance would need to be compensated for to be able to produce a color. Incorporating phase change materials that can switch the radiative cooling on and off at specific temperatures could also be a fruitful avenue of research, as human beings are most comfortable around room temperature.

Comprehensive experiments and research into the effects of humidity, dust, and pollutants in the air on the efficiency of radiative cooling should be done to understand how to optimize radiative cooling devices in different areas of the world. In some cases, high humidity causes the second atmospheric window to be completely closed, so a radiative cooling device that emits in that window would lose its efficiency in humid countries. The ability to switch between different selective emission responses at will would be a great improvement and step towards everyday use of energy-free radiative cooling. The biggest cooling effects have been shown under very precise conditions, where the losses due to conduction and convection of the surrounding air, and radiation from the surrounding surfaces

were minimized using a vacuum chamber. This proves that after the design of a radiative cooling device has been optimized in terms of reflection and emission spectra, there are still large gains to be had in the prevention of these parasitic losses from the surrounding areas.

The application of passive, energy-free all-day radiative cooling to structures, devices, and even clothing would be able to facilitate significant savings in global cooling energy consumption, which would not only be of great benefit for consumers, it would have definite positive effects on the prevention of air pollution and global warming.

Author Contributions: B.K., D.L. and T.B. wrote the paper. J.R. guided the entire paper.

Funding: This work was supported from the National Research Foundation of Korea (NRF) grant (NRF-2018M3D1A1058998) funded by the Ministry of Science and ICT (MSIT) of the Korean government.

Conflicts of Interest: The authors declare no conflict of interest.

References

1. Sanramouris, M.; Synnefa, M.; Karlessi, T. Using advanced cool materials in the urban built environment to mitigate heat islands and improve thermal comfort conditions. *Sol. Energy* **2011**, *85*, 1085–3102. [CrossRef]
2. Costanzo, V.; Evola, G.; Marletta, L. Cool roofs for passive cooling: Performance in different climates and for different insulation levels in Iraly. *Adv. Build. Energy Res.* **2013**, *7*, 155–169. [CrossRef]
3. Levinson, R.; Akbari, H.; Berdahl, P.; Wood, C.; Skilton, W.; Petersheim, J. A novel technique for the production of cool colored concrete tile and asphalt shingle roofing products. *Sol. Energy Mater. Sol. Cells* **2010**, *94*, 946–954. [CrossRef]
4. Trombe, F. Solar furnaces and their applications. *Sol. Energy* **1957**, *1*, 9–15. [CrossRef]
5. Ali, A.H.H.; Taha, I.M.S.; Ismail, I.M. Cooling of water flowing through a night sky radiator. *Sol. Energy* **1995**, *55*, 235–253. [CrossRef]
6. Al-Nim, M.; Tahat, M.M.; Al-Rashdan, M. A noght cold storage system enhanced by radiative cooling—A modified Australian cooling system. *Appl. Therm. Energy* **1999**, *19*, 1013–1026. [CrossRef]
7. Bao, H.; Yan, C.; Wang, B.; Fang, X.; Zhao, C.Y.; Ruan, X. Double-layer nanoparticle-based coatings for efficient terrestrial radiative cooling. *Sol. Energy Mater. Sol. Cells* **2017**, *168*, 78–84. [CrossRef]
8. Laatioui, S.; Benlattar, M.; Mazroui, M.; Saadouni, K. Zinc monochalcogenide thin films ZnX (X = S, Se, Te) as radiative cooling materials. *Optik* **2018**, *166*, 24–30. [CrossRef]
9. Roxana, F.; Pinar Mengüç, M. Materials for Radiative Cooling: A review. *Procedia Environ. Sci.* **2017**, *38*, 752–759. [CrossRef]
10. Bartoli, B.; Catalanotti, S.; Coluzzi, B.; Cuomo, V.; Silvestrini, V.; Troise, G. Nocturnal and diurnal performances of selective radiators. *Appl. Energy* **1977**, *3*, 267–286. [CrossRef]
11. Gansel, J.K.; Thiel, M.; Rill, M.S.; Decker, M.; Bade, K.; Saile, V.; von Freymann, G.; Linden, S.; Wegener, M. Gold Helix Photonic Metamaterial as Broadband Circular Polarizer. *Science* **2009**, *325*, 1513. [CrossRef] [PubMed]
12. Granqvist, C.G.; Hjortsberg, A. Radiative cooling to low temperatures: General considerations and application to selectively emitting SiO films. *J. Appl. Phys.* **1981**, *52*, 4205–4220. [CrossRef]
13. Hart, S.D.; Maskaly, G.R.; Temelkuran, B.; Prideaux, P.H.; Joannopoulos, J.D.; Fink, Y. External reflection from omnidirectional dielectric mirror fibers. *Science* **2002**, *296*, 510–513. [CrossRef] [PubMed]
14. Levinson, R.; Berdahl, P.; Akbari, H. Solar spectral optical properties of pigments—Part II: Survey of common colorants. *Sol. Energy Mater. Sol. Cells* **2005**, *89*, 351–389. [CrossRef]
15. Martin, M.; Berdahl, P. Characteristics of infrared sky radiation in the United States. *Sol. Energy* **1984**, *33*, 321–336. [CrossRef]
16. Min, W.-L.; Jiang, B.; Jiang, P. Bioinspired self-cleaning antireflection coatings. *Adv. Mater.* **2008**, *20*, 3914–3918. [CrossRef]
17. Weber, M.F.; Stover, C.A.; Gilbert, L.R.; Nevitt, T.J.; Ouderkirk, A.J. Giant birefringent optics in multilayer polymer mirrors. *Science* **2000**, *287*, 2451–2456. [CrossRef]
18. Inki, K.; Sunae, S.; Ahsan Sarwar, R.; Muhammad, Q.M.; Junsuk, R. Thermally robust ring-shaped chromium perfect absorber of visible light. *Nanophotonics* **2018**, *7*, 1827–1833. [CrossRef]

19. Dasol, L.; Sung Yong, H.; Yeonggyo, J.; Duc Minh, N.; Jeonghoon, C.; Gwanho, Y.; Jungho, M.; Jae Hyuck, L.; Jong, G.O.; Gun Young, J.; et al. Polarization-sensitive tunable absorber in visible and near-infrared regimes. *Sci. Rep.* **2018**, *8*, 12393. [CrossRef]
20. Ahsan, S.R.; Muhammad, Q.M.; Heonyeong, J.; Inki, K.; Junsuk, R. Tungsten-based ultrathin absorber for visible regime. *Sci. Rep.* **2018**, *8*, 2443. [CrossRef]
21. Gwanho, Y.; Sunae, S.; Minkyung, K.; Jungho, M.; Renmin, M.; Junsuk, R. Electrically tunable metasurface perfect absorber for infrared frequencies. *Nano Converg.* **2017**, *4*, 36. [CrossRef]
22. Nguyen, D.M.; Lee, D.; Rho, J. Control of light absorbance using plasmonic grating based perfect absorber at visible and near-infrared wavelengths. *Sci. Rep.* **2017**, *7*, 2611. [CrossRef] [PubMed]
23. Trevon, B.; Jungho, M.; Junsuk, R. Metasurfaces-based absorption and reflection control of light: Perfect absorbers and reflectors. *J. Nanomat.* **2017**, *2017*, 2361042. [CrossRef]
24. Bermel, P.; Boriskina, S.V.; Yu, Z.; Joulain, K. Control of radiative processes for energy conversion and harvesting. *Opt. Express* **2015**, *23*, A1533–A1540. [CrossRef] [PubMed]
25. Svetlana, V.B.; Martin, A.G.; Kylie, C.; Eli, Y.; Matthew, C.B.; Yoshitaka, O.; Stephan, L.; Talia, G.; Andriy, Z.; Mohammad, H.T.; et al. Roadmap on optical energy conversion. *J. Opt.* **2016**, *18*, 073004. [CrossRef]
26. Li, W.; Fan, S. Nanophotonic control of thermal radiation for energy applications. *Opt. Express* **2018**, *26*, 15995–16021. [CrossRef] [PubMed]
27. Chen, W.; Song, Y.; Zhang, L.; Liu, M.; Hu, X.; Zhang, Q. Thiophene-fused-heteroaromatic diones as promising NIR reflectors for radiative cooling. *Angew. Chem.* **2018**, *130*, 6397–6401. [CrossRef]
28. Raman, A.P.; Anoma, M.A.; Zhu, L.; Rephaeli, E.; Fan, S. Passive radiative cooling below ambient air temperature under direct sunlight. *Nature* **2014**, *515*, 540. [CrossRef] [PubMed]
29. Chen, Z.; Zhu, L.; Raman, A.; Fan, S. Radiative cooling to deep sub-freezing temperatures through a 24-h day–night cycle. *Nat. Commun.* **2016**, *7*, 13729. [CrossRef] [PubMed]
30. Jin-Woo, C.; Tae-Il, L.; Da-Som, K.; Keum-Hwan, P.; Yeong-Seok, K.; Sun-Kyung, K. Visible to near-infrared thermal radiation from nanostructured tungsten anntennas. *J. Opt.* **2018**, *20*, 09LT01. [CrossRef]
31. Zhou, H.; Xu, J.; Liu, X.; Zhang, H.; Wang, D.; Chen, Z.; Zhang, D. Bio-inspired photonic materials: Prototypes and structural effect designs for applications in solar energy manipulation. *Adv. Funct. Mater.* **2017**, *28*, 1705309. [CrossRef]
32. Shi, N.N.; Tsai, C.-C.; Camino, F.; Bernard, G.D.; Yu, N.; Wehner, R. Keeping cool: Enhanced optical reflection and radiative heat dissipation in Saharan silver ants. *Science* **2015**, *349*, 298–301. [CrossRef] [PubMed]
33. Ono, M.; Chen, K.; Li, W.; Fan, S. Self-adaptive radiative cooling based on phase change materials. *Opt. Express* **2018**, *26*, A777–A787. [CrossRef] [PubMed]
34. Fan, S.; Raman, A. Metamaterials for radiative sky cooling. *Nat. Sci. Rev.* **2018**, *5*, 132–133. [CrossRef]
35. Kecebas, M.A.; Menguc, M.P.; Kosar, A.; Sendur, K. Passive radiative cooling design with broadband optical thin-film filters. *J. Quant. Spectrosc. Radiat. Transf.* **2017**, *198*, 179–186. [CrossRef]
36. Zhao, D.; Martini, C.E.; Jiang, S.; Ma, Y.; Zhai, Y.; Tan, G.; Yin, X.; Yang, R. Development of a single-phase thermosiphon for cold collection and storage of radiative cooling. *Appl. Energy* **2017**, *205*, 1260–1269. [CrossRef]
37. Taylor, S.; Yang, Y.; Wang, L. Vanadium dioxide based Fabry-Perot emitter for dynamic radiative cooling applications. *J. Quant. Spectrosc. Radiat. Transf.* **2017**, *197*, 76–83. [CrossRef]
38. Kou, J.-L.; Jurado, Z.; Chen, Z.; Fan, S.; Minnich, A.J. Daytime radiative cooling using near-black infrared emitters. *ACS Photonics* **2017**, *4*, 626–630. [CrossRef]
39. Yang, P.; Chen, C.; Zhang, Z.M. A dual-layer structure with record-high solar reflectance for daytime radiative cooling. *Sol. Energy* **2018**, *169*, 316–324. [CrossRef]
40. Suichi, T.; Ishikawa, A.; Hayashi, Y.; Tsuruta, K. Performance limit of daytime radiative cooling in warm humid environment. *AIP Adv.* **2018**, *8*, 055124. [CrossRef]
41. Rephaeli, E.; Raman, A.; Fan, S. Ultrabroadband photonic structures to achieve high-performance daytime radiative cooling. *Nano Lett.* **2013**, *13*, 1457–1461. [CrossRef] [PubMed]
42. Zhu, L.; Raman, A.P.; Fan, S. Radiative cooling of solar absorbers using a visibly transparent photonic crystal thermal blackbody. *Proc. Natl. Acad. Sci. USA* **2015**, *112*, 12282–12287. [CrossRef] [PubMed]
43. Hossain, M.M.; Jia, B.; Gu, M. A Metamaterial emitter for highly efficient radiative cooling. *Adv. Opt. Mater.* **2015**, *3*, 1047–1051. [CrossRef]

44. Cui, Y.; Fung, K.H.; Xu, J.; Ma, H.; Jin, Y.; He, S.; Fang, N.X. Ultrabroadband light absorption by a sawtooth anisotropic metamaterial Slab. *Nano Lett.* **2012**, *12*, 1443–1447. [CrossRef] [PubMed]
45. Cui, Y.; He, Y.; Jin, Y.; Ding, F.; Yang, L.; Ye, Y.; Zhong, S.; Lin, Y.; He, S. Plasmonic and metamaterial structures as electromagnetic absorbers. *Laser Photon. Rev.* **2014**, *8*, 495–520. [CrossRef]
46. Ding, F.; Cui, Y.; Ge, X.; Jin, Y.; He, S. Ultra-broadband microwave metamaterial absorber. *Appl. Phys. Lett.* **2012**, *100*, 103506. [CrossRef]
47. Ji, D.; Song, H.; Zeng, X.; Hu, H.; Liu, K.; Zhang, N.; Gan, Q. Broadband absorption engineering of hyperbolic metafilm patterns. *Sci. Rep.* **2014**, *4*, 4498. [CrossRef]
48. Wu, D.; Liu, C.; Xu, Z.; Liu, Y.; Yu, Z.; Yu, L.; Chen, L.; Li, R.; Ma, R.; Ye, H. The design of ultra-broadband selective near-perfect absorber based on photonic structures to achieve near-ideal daytime radiative cooling. *Mater. Des.* **2018**, *139*, 104–111. [CrossRef]
49. Ikjoo, B.; Joonwon, K. Cost-effective laser interference lithography using a 405 nm AlInGaN semiconductor laser. *J. Micromech. Microeng.* **2010**, *20*, 055024. [CrossRef]
50. Choi, B.Y.; Pak, Y.; Kim, K.S.; Lee, K.H.; Jung, G.Y. Simultaneous fabrication of line defects-embedded periodic lattice by topographically assisted holographic lithography. *Nanoscale Res. Lett.* **2011**, *6*, 449. [CrossRef]
51. Seo, J.-H.; Park, J.H.; Kim, S.-I.; Park, B.J.; Ma, Z.; Choi, J.; Ju, B.-K. Nanopatterning by laser interference lithography: Applications to optical Devices. *J. Nanosci. Nanotechnol.* **2014**, *14*, 1521–1532. [CrossRef] [PubMed]
52. Matsuno, Y.; Sakurai, A. Perfect infrared absorber and emitter based on a large-area metasurface. *Opt. Mater. Express* **2017**, *7*, 618–626. [CrossRef]
53. Üstün, K.; Turhan-Sayan, G. Broadband LWIR and MWIR metamaterial absorbers with a simple design topology: Almost perfect absorption and super-octave band operation in MWIR band. *J. Opt. Soc. Am. B* **2017**, *34*, D86–D94. [CrossRef]
54. Zou, C.; Ren, G.; Hossain, M.M.; Nirantar, S.; Withayachumnankul, W.; Ahmed, T.; Bhaskaran, M.; Sriram, S.; Gu, M.; Fumeaux, C. Metal-loaded dielectric resonator metasurfaces for radiative cooling. *Adv. Opt. Mater.* **2017**, *5*, 1700460. [CrossRef]
55. Qu, Y.; Cai, L.; Luo, H.; Lu, J.; Qiu, M.; Li, Q. Tunable dual-band thermal emitter consisting of single-sized phase-changing GST nanodisks. *Opt. Express* **2018**, *26*, 4279–4287. [CrossRef] [PubMed]
56. Sun, K.; Riedel, C.A.; Wang, Y.; Urbani, A.; Simeoni, M.; Mengali, S.; Zalkovskij, M.; Bilenberg, B.; de Groot, C.H.; Muskens, O.L. Metasurface optical solar reflectors using AZO transparent conducting oxides for radiative cooling of spacecraft. *ACS Photonics* **2018**, *5*, 495–501. [CrossRef]
57. Hervé, A.; Drévillon, J.; Ezzahri, Y.; Joulain, K. Radiative cooling by tailoring surfaces with microstructures: Association of a grating and a multi-layer structure. *J. Quant. Spectrosc. Radiat. Transf.* **2018**, *221*, 155–163. [CrossRef]
58. Liu, T.; Takahara, J. Ultrabroadband absorber based on single-sized embedded metal-dielectric-metal structures and application of radiative cooling. *Opt. Express* **2017**, *25*, A612–A627. [CrossRef] [PubMed]
59. Wu, S.-R.; Lai, K.-L.; Wang, C.-M. Passive temperature control based on a phase change metasurface. *Sci. Rep.* **2018**, *8*, 7684. [CrossRef] [PubMed]
60. Jia, Z.-X.; Shuai, Y.; Li, M.; Guo, Y.; Tan, H.-P. Enhancement radiative cooling performance of nanoparticle crystal via oxidation. *J. Quant. Spectrosc. Radiat. Transf.* **2018**, *207*, 23–31. [CrossRef]
61. Zeyghami, M.; Goswami, D.Y.; Stefanakos, E. A review of clear sky radiative cooling developments and applications in renewable power systems and passive building cooling. *Sol. Energy Mater. Sol. Cells* **2018**, *178*, 115–128. [CrossRef]
62. Zhu, C.; Zhou, W.; Fang, J.; Ni, Y.; Fang, L.; Lu, C.; Xu, Z.; Kang, Z. Improved upconversion efficiency and thermal stability of NaYF4@SiO2 photonic crystal film. *J. Alloys Compd.* **2018**, *741*, 337–347. [CrossRef]
63. Gentle, A.R.; Smith, G.B. Radiative heat pumping from the earth using surface phonon resonant nanoparticles. *Nano Lett.* **2010**, *10*, 373–379. [CrossRef] [PubMed]
64. Huang, Z.; Ruan, X. Nanoparticle embedded double-layer coating for daytime radiative cooling. *Int. J. Heat Mass Transf.* **2017**, *104*, 890–896. [CrossRef]
65. Lu, Y.; Chen, Z.; Ai, L.; Zhang, X.; Zhang, J.; Li, J.; Wang, W.; Tan, R.; Dai, N.; Song, W. A Universal route to realize radiative cooling and light management in photovoltaic modules. *Solar. RRL* **2017**, *1*, 1700084. [CrossRef]

66. Gao, T.; Yang, Z.; Chen, C.; Li, Y.; Fu, K.; Dai, J.; Hitz, E.M.; Xie, H.; Liu, B.; Song, J.; et al. Three-dimensional printed thermal regulation textiles. *ACS Nano* **2017**, *11*, 11513–11520. [CrossRef] [PubMed]
67. Cai, L.; Song, A.Y.; Li, W.; Hsu, P.-C.; Lin, D.; Catrysse, P.B.; Liu, Y.; Peng, Y.; Chen, J.; Wang, H.; et al. Spectrally selective nanocomposite textile for outdoor personal cooling. *Adv. Mater.* **2018**, *30*, 1802152. [CrossRef]
68. Peng, Y.; Chen, J.; Song, A.Y.; Catrysse, P.B.; Hsu, P.-C.; Cai, L.; Liu, B.; Zhu, Y.; Zhou, G.; Wu, D.S.; et al. Nanoporous polyethylene microfibres for large-scale radiative cooling fabric. *Nat. Sustain.* **2018**, *1*, 105–112. [CrossRef]
69. Fu, Y.; Yang, J.; Su, Y.; Du, W.; Ma, Y. Daytime passive radiative cooler using porous alumina. *arXiv*, **2018**, arXiv:abs/1803.07906.
70. Wu, D.; Liu, C.; Liu, Y.; Yu, L.; Yu, Z.; Chen, L.; Ma, R.; Ye, H. Numerical study of an ultra-broadband near-perfect solar absorber in the visible and near-infrared region. *Opt. Lett.* **2017**, *42*, 450–453. [CrossRef]
71. Zhai, Y.; Ma, Y.; David, S.N.; Zhao, D.; Lou, R.; Tan, G.; Yang, R.; Yin, X. Scalable-manufactured randomized glass-polymer hybrid metamaterial for daytime radiative cooling. *Science* **2017**, *355*, 1062–1066. [CrossRef]
72. Zhang, X. Metamaterials for perpetual cooling at large scales. *Science* **2017**, *355*, 1023–1024. [CrossRef] [PubMed]
73. Atiganyanun, S.; Plumley, J.B.; Han, S.J.; Hsu, K.; Cytrynbaum, J.; Peng, T.L.; Han, S.M.; Han, S.E. Effective radiative cooling by paint-format microsphere-based photonic random media. *ACS Photonics* **2018**, *5*, 1181–1187. [CrossRef]
74. Mandal, J.; Fu, Y.; Overvig, A.C.; Jia, M.; Sun, K.; Shi, N.N.; Zhou, H.; Xiao, X.; Yu, N.; Yang, Y. Hierarchically porous polymer coatings for highly efficient passive daytime radiative cooling. *Science* **2018**, *362*, 315–319. [CrossRef] [PubMed]